J. Cent. South Univ. (2013) 20: 457–465
DOI: 10.1007/s11771-013-1507-x

Springer

Performance analysis and improvement of geothermal binary cycle power plant in oilfield

LI Tai-lu(李太禄)[1,2], ZHU Jia-ling(朱家玲) [1,2], ZHANG Wei(张伟) [1,2]

1. Key Laboratory of Efficient Utilization of Low and Medium Grade Energy of Ministry of Education (Tianjin University), Tianjin 300072, China;
2. Tianjin Geothermal Research and Training Center, School of Mechanical Engineering, Tianjin University, Tianjin 300072, China

Abstract: In order to improve the efficiency of a geothermal power plant, oil wells in the high water cut stage were used as geothermal wells, thereby improving the recovery ratio and economic benefit. A new function that reflects both the technical and economic performances was put forward and used as the objective function. An organic Rankine cycle (ORC) was analyzed through the energetic and exergetic analyses, and the reasons for low efficiency were pinpointed. Results indicate that geothermal water directly transferring heat to the working fluid reduces energy dissipation and increases cycle efficiencies. The net power output with an internal heat exchanger (IHE) is averagely 5.3% higher than that without an IHE. R601a and R601 can be used to replace R123 for geothermal water below 110 °C. Moreover, the modified ORC dramatically outperforms the actual one.

Key words: geothermal power generation; organic Rankine cycle; energetic and exergetic analyses; oilfield; internal heat exchanger

1 Introduction

The National Bureau of Statistics of China (NBSC) has estimated that China had a total energy consumption of 3.066 billion tons of standard coal in 2009, among which raw coal, crude oil, natural gas, and other forms account for 70.3%, 18.0%, 3.9%, and 7.8%, respectively [1]. The energy structure in China has been coal-dominated for a long time, thereby resulting in many serious environmental problems, such as global warming, ozone layer destruction and atmospheric pollution.

Among renewable energies, geothermal resources are the forms of energy being used today in various applications. The high temperature geothermal water is the most suitable for commercial production of electricity [2]. Geothermal binary power plants widen the scope of geothermal energy to generate electricity. For low and medium temperature geothermal water, binary cycle power plants can be used. Heat sources between 350 and 450 K reach a thermal efficiency ranging from 5% to 15% [3]. The main problem of low-temperature geothermal power generations is their poor economic efficiency because the drilling cost accounts for more than 50%.

Petroleum industry is one of the most significant energy industries. The average water cut of oilfields in China has reached 81.4% [4]. Oil wells with the water cut above 98% are considered to be unworthy further exploiting, but large quantities of oil are still unexploited. Lots of heat is needed for oil gathering and transportation, and oil boilers are mainly used as the heat source with a low efficiency, and the running costs increase with oil price [5]. Geothermal water over 85 °C can be used to replace oil boilers as the heat source of oil gathering and transportation heat tracing. However, geothermal water often exceeds 110 °C, and the stand-alone heat utilization will result in energy dissipation.

As mentioned above, the economic efficiency of oilfields in the high water cut stage is low. Traditional geothermal power plants show poor economic due to high drilling cost. Oil wells are used as geothermal wells, and the petroleum-associated water is used as the heat source. Geothermal water is first to generate electricity, and then it is used to heat up the backwater of oil gathering and transport the heat tracing. Besides power output and heating tracing, large quantities of crude oil can be recovered. Geothermal power plants in oilfield are much more competitive than the traditional ones, and the payback period can be greatly cut down. Geothermal

Foundation item: Project(2012AA052804) supported by the National High Technology Research and Development Program of China
Received date: 2012–01–04; **Accepted date:** 2012–05–04
Corresponding author: ZHANG Wei, PhD; Tel: +86–22–27401830; E-mail: zhangweitju@163.com

power generations using organic fluids in recovering low and medium temperature energy sources have attracted much attention in recent years. HETTIARACHCHI et al [6] presented a design criterion for organic Rankine cycle (ORC) utilizing low temperature geothermal source. The result showed that ammonia was preferable. BORSUKIEWICZ-GOZDUR and NOWAK [7] returned the stream of geothermal water from downstream of the evaporator for a repeated passage through that heat exchanger to maximize power output. Working fluids studied were R227ea, RC318, R236fa, R600a and R245ca. HEBERLE and BRÜGGEMANN [8] studied the series and parallel circuits of ORC and heat production for geothermal resources below 450 K by the second law analysis. The working fluids, isopentane, isobutene, R245fa and R227ea, were investigated. SALEH et al [9] used alkanes, fluorinated alkanes, ether and fluorinated ethers as working fluids in ORCs for geothermal power plants operating between 100 and 30 °C. DESAI and BANDYOPADHYAY [10] found that regeneration and turbine bleeding could improve the thermal efficiency of the basic ORC. KANOGLU and BOLATTTURK [11] investigated the exergetic efficiency and loss of each component of a binary cycle system driven by a liquid-dominated geothermal resource of 160 °C. YARI [12–13] analyzed different geothermal cycles and several dry fluids for the ORC. Results showed that R123 with IHE had the highest efficiency. GUO et al [14] investigated different pure organic fluids for the transcritical ORC driven by low temperature geothermal sources (80–120 °C). They recommended R125 as the supercritical fluid. HUA et al [15] presented and analyzed a simplified dual-pressure ammonia-water cycle with 85–110 °C heat source. WANG et al [16] investigated several working fluids for low temperature heat recovery. The results showed that R123 was the best choice. WANG et al [17] established an optimized mathematical model to improve the performance of the power generation driven by low-temperature waste heat.

In this work, an actual geothermal power plant in an oilfield was analyzed based on the data of the power plant. The objective was to improve the efficiency of the plant. Firstly, the reasons for low efficiency were pinpointed. Then, the system performance was calculated numerically through the energetic and exergetic analyses. Finally, a new objective function was put forward and used to optimize the ORC system, and the most suitable working fluid was obtained.

2 System description and modeling

2.1 System description

Figure 1 shows the schematic diagram of an actual geothermal power plant in an oilfield. The system consists of a plate heat exchanger (PHE), a hot water pump, an evaporator, a turbine, a condenser, a feed pump, a cooling pump, and a cooling tower. Geothermal water transfers heat to water. The organic fluid absorbs heat from the water to generate high-pressure vapor in the evaporator, then the vapor flows into the turbine and its enthalpy is converted into work. The vapor exits the turbine and it is led to the condenser where it is liquefied by cooling water. The liquid available at the condenser outlet is pressurized and flows into the evaporator, then a new cycle begins. The ORC can be identified as 1→2→3→4→1. Figure 2 shows the actual ORC power generation.

The schematic diagram and the corresponding *T*–*S* diagram of the modified ORC system are shown in Figs. 2 and 3. For the modified power plant, geothermal water directly transfers heat to the working fluid without intermediate heat carrier, so the PHE and the hot water pump are dismantled whereas an IHE is employed. The modified ORC can be identified as 1→2a→2→3→4→4a→1.

The advantages of the modified ORC system are shown as follows: on one hand, direct heat transfer between geothermal water and working fluid can prevent additional heat loss and the temperature decrease of the heat source, and adding an internal heat exchanger (IHE) can reduce the heat addition to the working fluid and lead to a higher efficiency. On the other hand, the dismantling of the hot water pump can make full use of the excessive pressure of geothermal water, thereby decreasing the initial investment and operating cost.

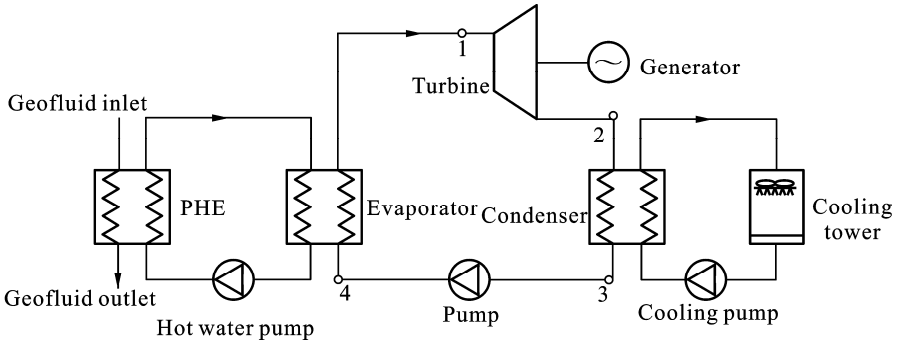

Fig. 1 Schematic diagram of actual ORC geothermal power plant

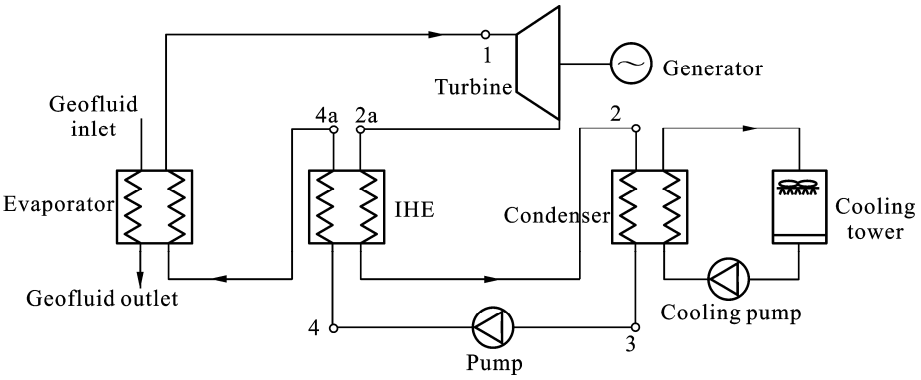

Fig. 2 Schematic diagram of modified ORC geothermal power plant

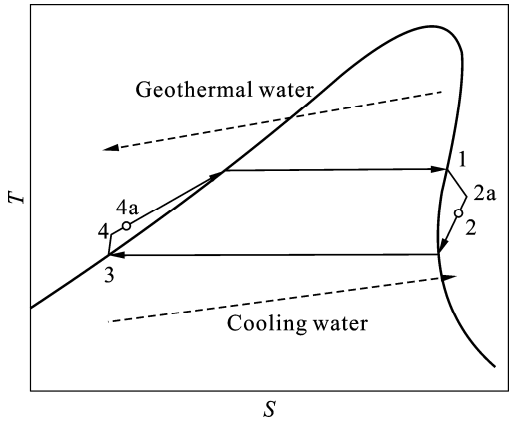

Fig. 3 *T*–*S* diagram of modified ORC

2.2 Modeling

The energy and exergy analyses based on the first and second laws of thermodynamics were evaluated for the working fluids investigated. For simplicity, the following hypotheses were made:

(1) Geothermal power plants operate steadily.

(2) Saturated vapor is considered at the turbine inlet and saturated liquid at the condenser exit.

(3) The kinetic and potential energy changes are negligible.

(4) The temperature and friction losses are neglected.

The mathematical model is expressed by

$$W_{se}=m(h_1-h_2) \tag{1}$$

where W_{se} is the mechanical work of the screw expander, m is the mass flow rate of the working fluid, and h_1 and h_2 are the incoming and outgoing flow enhalpies of the screw expander, respectively.

$$I_{se}=mT_0(s_2-s_1) \tag{2}$$

where I_{se} is the irreversibility for the screw expander, T_0 is the ambient temperature, and s_1 and s_2 are the incoming and outgoing flow entropies of the screw expander, respectively.

$$Q_c=m(h_2-h_3) \tag{3}$$

$$I_c=mT_0[(s_3-s_2)-(h_3-h_2)/T_L] \tag{4}$$

$$W_{pc}=m\Delta p_c/(\eta_{pc}\rho) \tag{5}$$

where Q_c is the absolute value of the heat transfer in the condenser, H_3 is the enthalpy at the condenser outlet, I_c is the irreversibility of the condenser, S_3 is the entropy at the condenser outlet, T_L is the temperature of heat carrying fluid in the condenser, W_{pc} is the power of the cooling pump, Δp_c is the pressure drop of the cooling water, η_{pc} is the isentropic efficiency of the cooling pump, and ρ is the density of water.

$$W_p=m(h_4-h_3) \tag{6}$$

$$I_p=mT_0(s_4-s_3) \tag{7}$$

where W_p represents the power of the pump, I_p is the irreversibility for the pump, and h_4 and s_4 are the enthalpy and entropy at the outlet of the pump, respectively.

$$Q_e=m(h_1-h_4) \tag{8}$$

$$I_e=mT_0[(s_1-s_4)-(h_1-h_4)/T_H] \tag{9}$$

$$W_{pe}=m\Delta p_e/(\eta_{pe}\rho) \tag{10}$$

where Q_e represents the absolute value of the heat transfer in the evaporator, I_e is the irreversibility for the evaporator, T_H is the temperature of the heat source in the evaporator, W_{pe} is the pump power of the hot water, Δp_e is the pressure drop of hot water, and η_{pe} is the isentropic efficiency of the hot water pump.

$$I_{tot}=I_{se}+I_c+I_p+I_e \tag{11}$$

$$W_{net}=\eta_g W_{se}-W_p-W_{pc}-W_{pe} \tag{12}$$

$$\eta_{th}=W_{net}/Q_e \tag{13}$$

$$\eta_{ex}=W_{net}/(W_{net}+I_{tot}) \tag{14}$$

where I_{tot} is the total irreversibility, W_{net} is the net power output, η_g is the efficiency of the generator, and η_{th} and η_{ex} are the thermal and exergetic efficiencies, respectively.

Numerical correlations were used to calculate the

heat transfer coefficient in the evaporator as follows [18–21].

3 Validation

Numerical solution is validated with the data of SALEH et al [9] for various working fluids based ORC without regenerators in the same operating conditions. The results of present solutions show very good agreement with the results in Ref. [9] as given in Table 1. The differences mainly derive from the selection of equation of state (EOS) that the BACKONE EOS was adopted in Ref. [9] while the fundamental EOS was selected in this work.

4 Results and discussion

4.1 Analysis of basic ORC

Table 2 gives the parameters of an actual plant, which derive from an actual geothermal binary power plant in an oilfield.

Table 3 gives the thermal and exergetic efficiencies in references. It can be seen from Tables 2 and 3 that the efficiencies of the actual power plant are lower than those in the references.

Figure 4 shows the irreversibility of different components for the actual ORC. It can be seen that the irreversibility in the evaporator is the highest, reaching 238.1 kW, followed by the condenser. The irreversibility in the PHE is almost the same as in the turbine, about 135 kW. The irreversibility caused by the feed pump is the lowest, only 3.03 kW. The PHE results in heat dissipation. More seriously, it decreases the heat source temperature, which is extremely disadvantageous to low temperature geothermal resources. Therefore, the more efficient evaporator should be used to dismantle the PHE.

4.2 Selection of working fluids

The selection of working fluids has a significant effect on the system performance. The working fluids

Table 1 Validation of numerical model with previous published data for various fluids-based ORC

Substance	T_{cri}/°C	P_{cri}/MPa	T_1/°C	T_3/°C	P_e/MPa	P_c/MPa	m/(kg·s^{-1})	V_1/(m^3·s^{-1})	V_1/V_2	η_{th}/%	Source
R125	66.18	3.630	40.06	30.00	2.000	1.564	400.37	2.878	1.270	2.32	[9]
R125	66.18	3.630	40.06	30.00	2.000	1.564	400.37	2.834	1.360	2.35	Present work
R290	96.65	4.250	57.14	30.00	2.000	1.079	48.776	1.063	1.667	5.91	[9]
R290	96.65	4.250	57.14	30.00	2.000	1.079	48.776	1.049	1.764	5.81	Present work
R134a	101.03	4.056	67.75	30.00	2.000	0.772	68.55	0.656	2.357	7.74	[9]
R134a	101.03	4.056	67.75	30.00	2.000	0.772	68.55	0.639	2.483	7.48	Present work

Table 2 Parameters of actual ORC power plant in oilfield

Parameter	Value/Type	Parameter	Value/Type
Geothermal water inlet temperature/°C	110	Turbine exhaust pressure/MPa	0.16
Geothermal water outlet temperature/°C	90	Working fluid	R123
Geothermal flow rate/(m^3·h^{-1})	250	Working fluid flow rate/(m^3·h^{-1})	107
Inlet water temperature of evaporator/°C	100	Outlet cooling water temperature/°C	28
Outlet water temperature of evaporator/°C	80	Outlet working fluid temperature of condenser/°C	38
Water flow rate/(m^3·h^{-1})	250	Net power output/kW	270
Turbine inlet temperature/°C	87	Thermal efficiency/%	4.65
Turbine inlet pressure/MPa	0.58	Exergetic efficiency/%	25.76
Turbine exhaust temperature/°C	42		

Table 3 Thermal and exergetic efficiencies in References

Item	η_{th} /%	η_{ex} /%	Source
Otake pilot binary geothermal power plant	12.9	53.9	[22]
Heber SIGC geothermal power plant	13.2	50.7	[22]
Húsavík Kalina cycle power plant	10.6	41.4	[22]
Simple ORC of R123	7.65	38.76	[12]
Simple ORC of *n*-pentane	7.376	37.37	[12]
R141b in b2 cycle	17	—	[23]
R600a in o3 cycle	15.1	—	[23]
R601a in o2 cycle	15.9	—	[23]
ORC	20.6	35.5	[24]
Kalina	24.1	43.0	[24]
Dual-level of geothermal power plant	8.9	29.1	[25]

used to simulate the performance of ORC system are listed in Table 4. The normal boiling point ranges from –11.96 to 47.59 °C.

4.3 Comparison of ORC with and without PHE

The relevant parameters used in the simulation were derived from the aforementioned actual binary geothermal power plant in oilfield in China, as listed in Table 5. The working fluid is considered saturated at the turbine inlet and saturated liquid at the condenser outlet.

Table 6 shows the optimal evaporating temperature for working fluids with and without PHE. It can be seen that the maximum net power output for the ORC without PHE is averagely 20% higher than that with PHE, For temperature ranges from 82 to 87°C and RC318 shows the highest net power output followed by R601a, whereas it ranges from 92 to 99°C for the cycle without a PHE, and R601a shows the highest net power output followed by RC318. R124 shows the lowest net power in both cases.

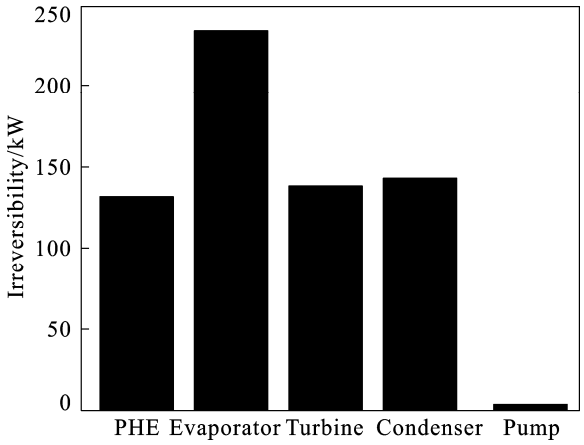

Fig. 4 Irreversibility of different components for actual ORC power plant

Therefore, the more efficient evaporator should be used to dismantle the PHE, thereby improving the cycle performance.

4.4 Comparison of ORC with and without IHE

Table 7 shows the net power output versus the evaporating temperature with and without an IHE. The net power output for the ORC with an IHE is averagely 5.30% higher than that without IHE, because the working fluid with high pressure absorbs a small fraction of condensation heat before entering the evaporator.

Table 4 Thermodynamic properties of working fluids

Substance	Physical data				Environmental data			Source	Type of fluid
	M/(g·mol^{-1})	T_b /°C	T_{cri}/°C	P_{cri}/MPa	ALT/a	ODP	GWP/100a		
R124	136.48	–11.96	122.28	3.624	5.8	0.02	609	[26]	Isentropic
R600a	58.12	–11.67	134.67	3.640	0.02	0	~20	[27]	Isentropic
RC318	200.03	–5.98	115.23	2.778	3200	0	10,250	[28]	Isentropic
R236fa	152.04	–1.44	124.92	3.200	240	0	9810	[29]	Isentropic
R600	58.12	–0.55	151.98	3.796	0.02	0	~20	[30]	Isentropic
R114	170.92	3.59	145.68	3.257	300	1.00	1,0040	[28]	Isentropic
R245fa	134.05	14.90	154.05	3.640	7.6	0	1030	[29]	Isentropic
R601a	72.15	27.80	187.2	3.380	0.01	0	~20	[29]	Dry
R123	152.93	27.82	183.68	3.662	1.3	0.02	77	[29]	Isentropic
R141b	116.95	32.05	206.81	4.460	9.3	0.12	725	[28]	Isentropic
R601	72.15	36.1	196.6	3.257	0.01	0	~20	[29]	Dry
R113	187.38	47.59	214.06	3.392	85	1.00	6130	[29]	Isentropic

ALT：Atmosphere life time; ODP: Ozone depletion potential; GWP: Global warming potential

Table 5 Parameters used in simulation under saturated conditions

Parameter	Value
Geothermal water inlet temperature/°C	110
Geothermal water outlet temperature/°C	90
Geothermal water flow rate/($m^3 \cdot h^{-1}$)	250
Water temperature at the evaporator inlet/°C	100
Water temperature at the evaporator outlet/°C	80
Water flow rate/($m^3 \cdot h^{-1}$)	250
Turbine exhaust temperature/°C	42
Turbine exhaust pressure/MPa	0.16
Cooling water temperature at condenser inlet/°C	28
Cooling water temperature at condenser outlet/°C	38
Working fluid temperature at condenser outlet/°C	33
Working fluid temperature at evaporator inlet with IHE/°C	40
Pinch point temperature difference/°C	3
Ambient temperature/°C	25
Efficiency of generator/%	90
Efficiency of feed pump/%	60
Efficiency of screw expander/%	60
Efficiency of hot water pump/%	75
Efficiency of cooling pump/%	75
Pump head of hot water pump/m	20
Pump head of cooling pump/m	20

The working fluids show similar variation trends, R601a is taken as an example to simplify the analysis. The log mean temperature difference (LMTD) and the evaporator heat exchange area of the cycle without an IHE are lower than those with an IHE for the evaporating temperature lower than 65 °C, as opposed to the evaporating temperature higher than 65 °C. The irreversibility of the evaporator and the condenser for the cycle with an IHE is lower than that without IHE, because the IHE reduces the condensation heat load and decreases the mean temperature difference between geothermal water and working fluid in the evaporator. As for the pump and the turbine, the irreversibility for the cycle with an IHE is higher than that without IHE, because an IHE increases the mass flow rate of the working fluid. The irreversibility is proportional to the mass flow rate with other parameters remaining steady. Therefore, the ORC with an IHE effectively increases the system performance.

Table 6 Optimal evaporating temperature for working fluids with and without PHE

Substance	PHE	$T_{e,opt}$ /°C	W_{net} /kW
R124	With	84	223.3
	Without	96	258.0
R600a	With	84	302.4
	Without	95	364.7
RC318	With	87	424.2
	Without	99	476.8
R236fa	With	85	324.5
	Without	97	377.5
R600	With	83	307
	Without	94	378.2
R114	With	84	373.2
	Without	95	452.8
R245fa	With	83	335.7
	Without	95	417.2
R601a	With	83	384
	Without	94	483.9
R123	With	82	302.7
	Without	93	380.6
R141b	With	82	260.7
	Without	92	330.6
R601	With	82	377.3
	Without	93	474.6
R113	With	82	360.9
	Without	93	453.4

Table 7 Optimal evaporating temperature for working fluids with and without IHE

Substance	IHE	$T_{e,opt}$/°C	W_{net}/kW
R124	Without	96	258.0
	With	96	271.5
R600a	Without	95	364.7
	With	95	382.3
RC318	Without	99	476.8
	With	98	504.3
R236fa	Without	97	377.5
	With	96	395.1
R600	Without	94	378.2
	With	94	394.7
R114	Without	95	452.8
	With	95	471.5
R245fa	Without	95	417.2
	With	94	433.6
R601a	Without	94	483.9
	With	93	495.9
R123	Without	93	380.6
	With	93	394.3
R141b	Without	92	330.6
	With	92	342.9
R601	Without	93	474.6
	With	93	494.2
R113	Without	93	454.4
	With	93	464.5

4.5 Optimization of ORC with IHE but without PHE

Figure 5 shows the LMTD versus the evaporating temperature for the ORC with an IHE but without a PHE. It can be seen that the LMTD decreases with the evaporating temperature. For the evaporating temperature lower than 85 °C, R141b has the highest LMTD followed by R113, and RC318 has the lowest LMTD. For the evaporating temperature higher than85 °C, RC318 has the highest LMTD whereas R141b has the lowest LMTD.

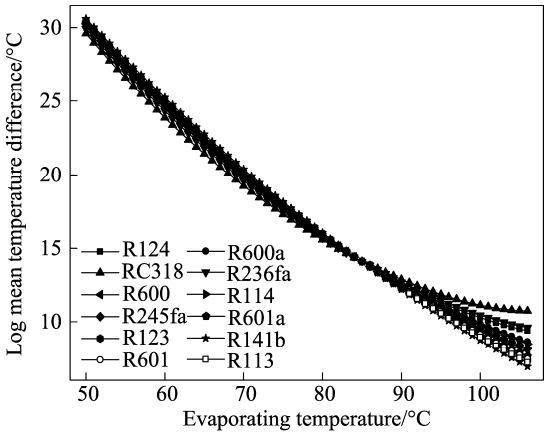

Fig. 5 LMTD versus evaporating temperature for ORC with IHE but without PHE

Figure 6 shows the heat exchange area of the evaporator versus the evaporating temperature for the ORC with an IHE but without a PHE. It can be seen that the heat transfer area of the evaporator increases with the evaporating temperature. For the evaporating temperature lower than 85 °C, RC318 has the highest heat transfer area followed by R236fa, and R141b has the lowest heat exchange area. For the evaporating temperature higher than 85 °C, R141b has the highest heat exchange area whereas RC318 has the lowest heat exchange area. It can be concluded from Figs. 5 and 6 that the variation trend is quite contrary, due to the fact that the evaporator heat exchange area is inversely proportional to the LMTD for a specific evaporating temperature.

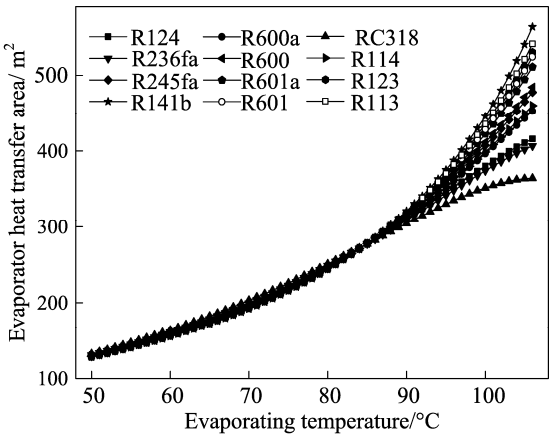

Fig. 6 Evaporator heat transfer area versus evaporating temperature for ORC with IHE but without PHE

Figure 7 shows the net power output versus the evaporating temperature for the ORC with an IHE but without a PHE. It can be seen that the net power output first increases and then decreases after reaching the maximum. RC318 always shows the highest net power output except that R601a has the highest net power output for the evaporating temperature between 92 and 93 °C whereas R124 invariably exhibits the lowest net power output. There exists an optimal maximum evaporating temperature maximizing the net power output, which varies with working fluid. RC318 presents the maximum net power output of 504.3 kW with 1.69% higher net power output than R601a which shows the second highest net power output.

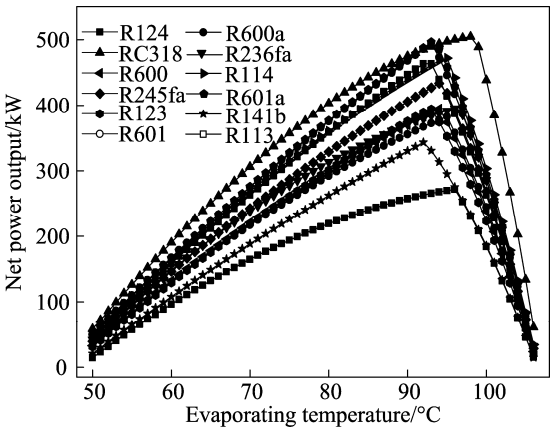

Fig. 7 Net power output versus evaporating temperature for ORC with IHE but without PHE

Figure 8 shows the ratio of the net power output to the heat transfer area of the evaporator versus the evaporating temperature for the ORC with an IHE but without a PHE. It can be seen that the ratio of the net power output to the heat transfer area of the evaporator

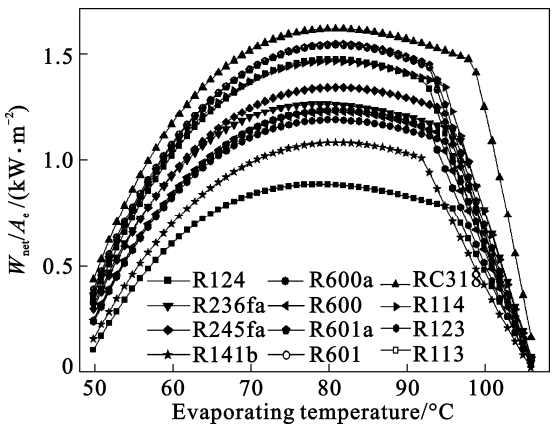

Fig. 8 Ratio of net power output to evaporator heat transfer area versus evaporating temperature for ORC with IHE but without PHE

first increases and then decreases. The slope suddenly decreases after the turning point and the ratio approximately linearly reduces. There exists an optimal evaporating temperature maximizing the ratio of the net power output to the heat transfer area of the evaporator. The ratio reaches its maximum with an evaporating temperature of about 81 °C, which is consistent for the working fluids investigated. The maximum ratio for RC318 is the highest, reaching 1.61 kW/m^2 followed by R601a, R601, and R114. R114 presents the lowest ratio for the evaporating temperature lower than 96 °C whereas R141b is the lowest for the evaporating temperature higher than 96 °C.

The efficiencies only reflect system technical performance but do not reflect system economic performance, whereas the ratio of the net power output to the evaporator heat exchange area is just the opposite, and both of them are partial. Taken the technical and economic performances into consideration, a new function f_{obj} is put forward and used as the objective function shown as follows:

$$f_{obj}=(W_{net}/W_{net,o})\cdot(\eta_{th}/\eta_{th,o})\cdot(A_o/A) \quad (15)$$

where A is the heat transfer area in the evaporator, and subscribe "o" stands for the original actual geothermal power plant.

Figure 9 shows the objective function versus the evaporating temperature for the ORC with an IHE but without a PHE. It can be seen that the objective function first increases and then decreases after reaching the maximum. All the working fluids reach their maximum at the turning point except that R124 and RC318 get the maximum at the evaporating temperature lower than the turning point. RC318 shows the highest objective function within the scope of this work.

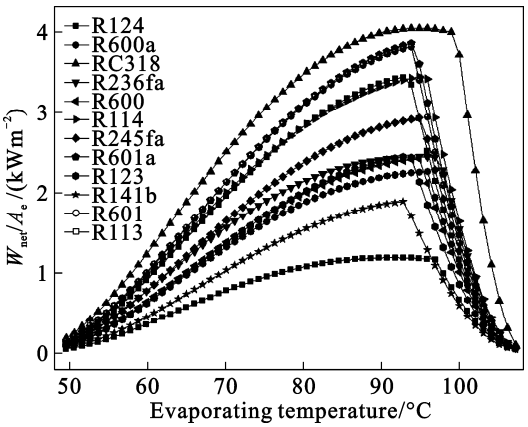

Fig. 9 Objective function versus evaporating temperature for ORC with IHE but without PHE

The maximum objective function and the corresponding parameters of the ORC with an IHE but without a PHE are shown in Table 8. RC318 has the highest objective function value reaching 4.04 followed by R601a and R601; whereas R124 presents the lowest objective function value.

Table 8 Maximum objective function and optimal evaporating temperature for ORC with IHE but without PHE

Substance	$f_{obj,max}$	T_e /°C	P_e /MPa	W_{net} /kW	A /m^2
R124	1.152	91	1.985	260.3	317.3
R600a	2.238	95	1.779	382.3	352.5
RC318	4.040	94	1.816	493.4	325.3
R236fa	2.423	94	1.708	387.9	335.2
R600	2.401	94	1.356	393.7	350.2
R114	3.431	94	1.246	468.1	344.7
R245fa	2.913	94	1.102	433.6	348.4
R601a	3.854	93	0.605	495.9	344.4
R123	2.426	92	0.655	389.4	337.4
R141b	1.861	92	0.564	342.9	453.1
R601	3.808	93	0.503	494.2	346.2
R113	3.428	92	0.362	463.5	338.3

4.6 Overall analysis of working fluids

The previous analyses aim at increasing the tech-economic performance of the ORC plant with a view of the working fluid thermodynamic properties. Other parameters should also be considered, such as low ODP, low GWP, non-flammable, non-toxic and non-corrosive. Considering the environmental characteristics (ODP value less than 0.2, GWP value less than 1 500), R113 is now banned and R114 has now been phased out due to their high ODP values. RC318 and R236fa should be abandoned because of their high GWP values. In addition, R123 is now being phased out.

Finally, R601a followed by R601 can be used as the most suitable working fluids for low temperature binary cycle geothermal plants with geothermal water lower than 110 °C.

5 Conclusions

1) Direct heat transfer between geothermal water and the working fluid in the evaporator is preferable, improving the system efficiency by about 20.0% compared with indirect heat transfer.

2) The IHE recovering a portion of condensation heat not only lowers the heat load in the condenser but also reduces the heat absorption of unit mass working fluid in the evaporator, thereby increasing the net power output by about 5.3%.

3) R601a and R601 can be used to replace R123 as the working fluid of geothermal power generation for geothermal water below 110 °C.

4) The modified ORC plant outperforms the actual

one evidently, which can be widely used in engineering applications.

References

[1] National Bureau of Statistics of China. China statistical abstract 2010 [R]. Beijing: China Statistics Press, 2010. (in Chinese)

[2] BARBIER E. Geothermal energy technology and current status: An overview [J]. Renewable and Sustainable Energy Review, 2002, 6(1/2): 3–65.

[3] DRESCHER U. Optimierungspotenzial des Organic Rankine Cycle für geothermische und biomassebefeuerte Wärmequellen [D]. Berlin: University Bayreuth, 2008. (in Chinese)

[4] HAN Gang. Study on computational method of the water flooded layer aqueous saturation in high water cut stage [D]. Daqing: Daqing Petroleum Institute, 2008. (in Chinese)

[5] TIAN Yu-jiang. Technical research of using geothermal water for heat tracing system in gathering system of oil field [D]. Dongying: China University of Petroleum, 2009. (in Chinese)

[6] HETTIARACHCHI H D M, GOLUBOVIC M, WOREK W M, IKEGAMI Y. Optimum design criteria for an organic Rankine cycle using low-temperature geothermal heat sources [J]. Energy, 2007, 32(9): 1698–1706.

[7] BORSUKIEWICZ-GOZDUR A, NOWAK W. Maximising the working fluid flow as a way of increasing power output of geothermal power plant [J]. Applied Thermal Engineering, 2007, 27: 2074–2078.

[8] HEBERLE F, BRÜGGEMANN D. Exergy based fluid selection for a geothermal organic Rankine cycle for combined heat and power generation [J]. Applied Thermal Engineering, 2010, 30(11/12): 1326–1332.

[9] SALEH B, KOGLBAUER G, WENDLAND M, FISCHER J. Working fluids for low temperature organic Rankine cycles [J]. Energy, 2007, 32(7): 1210–1221.

[10] DESAI N B, BANDYOPADHYAY S. Process integration of organic Rankine cycle [J]. Energy, 2009, 34(10): 1674–1686.

[11] KANOGLU M, BOLATTTURK A. Performance and parametric investigation of a binary geothermal power plant by exergy [J]. Renewable Energy, 2008, 33(11): 2366–2374.

[12] YARI M. Exergetic analysis of various types geothermal power plants [J]. Renewable Energy, 2010, 35(1): 112–121.

[13] YARI M. Performance analysis of the different organic Rankine cycles (ORCs) using dry fluids [J]. International Journal of Exergy, 2009, 6(3): 23–42.

[14] GUO T, WANG H X, ZHANG S J. Comparative analysis of natural and conventional working fluids for use in transcritical Rankine cycle using low-temperature geothermal source [J]. International Journal of Energy Research, 2011, 35(6): 530–544.

[15] HUA Jun-ye, CHEN Ya-ping, LIU Hua-jin, WU Jia-feng. Thermodynamic analysis of simplified dual-pressure ammonia-water absorption power cycle [J]. Journal of Central South University, 2012, 19(3): 797–802.

[16] WANG Zhi-qi, ZHOU Nai-jun, LUO Liang, ZHANG Jia-qi, TONG Dao-hui. Comparison of thermodynamic performance for waste heat power generation system with different low temperature working fluids [J]. Journal of Central South University: Science and Technology,, 2010, 41(6): 2424–2429. (in Chinese)

[17] WANG Zhi-qi, ZHOU Nai-jun, GUO Jing, WANG Xiao-yuan. Parametric optimization of low-temperature waste heat power generation system by simulated annealing algorithm [J]. Journal of Central South University: Science and Technology, 2012, 43 (1): 366–371. (in Chinese)

[18] MARTIN H. A theoretical approach to predict the performance of chevron-type plate heat exchangers [J]. Chemical Engineering and Processing, 1996, 35(4): 301–310.

[19] KHAN T S, KHAN M S, CHYU M C, AYUB Z H. Experimental investigation of single phase convective heat transfer coefficient in a corrugated plate heat exchanger for multiple plate configurations [J]. Applied Thermal Engineering, 2010, 30(8/9): 1058–1065.

[20] COOPER M G. Heat flows rates in saturated pool boiling: A wide ranging examination using reduced properties, advances in heat transfer [M]. Florida: Academic Press, 1984.

[21] PALM B, CLAESSON J. Plate heat exchanger: calculation methods for single and two-phase flow [J]. Heat Transfer Engineering, 2006, 27(4): 88–98.

[22] DIPIPPO R. Second Law assessment of binary plants generating power from low temperature geothermal fluids [J]. Geothermics, 2004, 33(4): 565–586.

[23] ARSLAN O, KOSE R. Exergoeconomic optimization of integrated geothermal system in Simav, Kutahya [J]. Energy Conversion and Management, 2010, 51(4): 663–676.

[24] WANG Jiang-feng, DAI Yi-ping, GAO Lin. Exergy analyses and parametric optimizations for different cogeneration power plants in cement industry [J]. Applied Energy, 2009, 86(6): 941–948

[25] KANOGLU M. Exergy analysis of a dual-level binary geothermal power plant [J]. Geothermics, 2002, 31(6): 709–724

[26] de VRIES B, TILLNER-ROTH R, BAEHR H D. Thermodynamic properties of HCFC 124 [C]// Nineteenth international congress of refrigeration. The Hague: International Institution of Refrigeration, 1995: 582–589.

[27] MIYAMOTO H, WATANABE K. A thermodynamic property model for fluid-phase isobutene [J]. International Journal of Thermophysics, 2002, 23(2): 477–499.

[28] PLATZER B, POLT A, MAURER G. Thermophysical properties of refrigerants [M]. Berlin: Springer-Verlag, 1990.

[29] CALM J M, HOURAHAN GC. Refrigerant data update [J]. Heating/Piping/Air Conditioning Engineering, 2007, 79(1): 50–64.

[30] MIYAMOTO H, WATANABE K. Thermodynamic property model for fluid-phase n-butane [J]. International Journal of Thermophysics, 2001, 22(2): 459–475.

(Edited by HE Yun-bin)